Available online at www.sciencedirect.com
ScienceDirect
Journal of the European Ceramic Society 29 (2009) 2999–3006
www.elsevier.com/locate/jeurceramsoc

Mechanochemical reaction in the K_2CO_3–Nb_2O_5 system

Tadej Rojac [a,*], Marija Kosec [a], Maria Połomska [b], Bożena Hilczer [b], Primož Šegedin [c], Andreja Bencan [a]

[a] *Jožef Stefan Institute, Jamova cesta 39, 1000 Ljubljana, Slovenia*
[b] *Institute of Molecular Physics, Polish Academy of Sciences, M. Smoluchowskiego 17, 60-179 Poznań, Poland*
[c] *Faculty of Chemistry and Chemical Technology, University of Ljubljana, Aškerčeva 5, 1000 Ljubljana, Slovenia*

Received 19 December 2008; received in revised form 7 April 2009; accepted 16 April 2009
Available online 26 May 2009

Abstract

We studied the mechanochemical synthesis of $KNbO_3$, starting from a powder mixture of K_2CO_3 and Nb_2O_5. The milling experiments were designed with different ball-impact energies in order to investigate the mechanochemical reactions. X-ray diffraction, thermogravimetric analysis, infrared spectroscopy, Raman spectroscopy and transmission electron microscopy were used to characterize the samples. Based on the results, we propose a mechanism for the mechanochemical reaction between K_2CO_3 and Nb_2O_5. The first stage of the reaction is characterized by the formation of an amorphous carbonato complex, which decomposes after prolonged milling at higher ball-impact energy giving rise to the crystallization of $KNbO_3$ and other niobate phases with a molar ratio K/Nb < 1. The reaction course is discussed and compared with the Na_2CO_3–Nb_2O_5 system.

Keywords: Milling; Niobates; Mechanochemical synthesis

1. Introduction

The increasing demands for environmentally acceptable piezoelectric oxide materials have recently triggered a worldwide search for lead-free piezoelectrics. One of the most promising groups of materials is based on the (K,Na)NbO_3 (KNN) solid solution.[1,2] Such materials are usually prepared by a conventional solid-state synthesis route, where multiple calcinations at elevated temperatures with intermediate wet-milling steps are applied. However, in addition to the problem of a large number of processing steps, a homogeneous mixture of the components is difficult to achieve.[3] Moreover, the high temperatures involved can also increase the volatilization of alkali oxides, giving rise to stoichiometry variations and the formation of secondary phases.[4] For these reasons, alternative synthesis methods need to be explored.

Mechanochemical synthesis has recently received a lot of interest for the processing of complex perovskite materials.[5] Its main advantage lies in the possibility of preparing nanopowders at low temperatures, directly by a simple milling procedure. Due to their complex nature, however, the mechanisms of mechanochemical reactions are presently not yet fully understood. Systematic studies on reaction mechanisms have been made for systems involving oxides[6–10] and mixtures of hydroxides and oxides[11–14] as reagents. In the first case, based on the mechanochemical synthesis of various complex oxides, such as for example $Pb(Mg_{1/3}Nb_{2/3})O_3$ and $0.65Pb(Mg_{1/3}Nb_{2/3})O_3$–$0.35PbTiO_3$, a nucleation-and-growth mechanism from the amorphous phase was proposed.[6,9] In the second case, where hydroxyl groups are involved, the mechanochemical interaction between the reagents proceeds via a superficial acid–base reaction, which results in dehydration and formation of a heterobridging bond.[14] However, in contrast to these systematic studies, poor data exist for systems in which a carbonate compound is involved in the mechanochemical reaction.[15]

In our previous study on the reaction mechanism in the Na_2CO_3–Nb_2O_5 system we showed that in the initial stage of milling, before the formation of $NaNbO_3$, an amorphous carbonato complex is formed as a result of the mechanochemical interaction between the two reagents.[15] By designing the milling experiments using a milling map,[16] we studied in detail the mechanochemical formation of $NaNbO_3$, characterized by a nucleation from the amorphous phase.[17] This is in agreement

* Corresponding author. Tel.: +386 1 477 38 34; fax: +386 1 477 38 87.
E-mail address: tadej.rojac@ijs.si (T. Rojac).

0955-2219/$ – see front matter © 2009 Elsevier Ltd. All rights reserved.
doi:10.1016/j.jeurceramsoc.2009.04.017

with the mechanisms proposed also by other researchers.[6,9] However, all the findings relate only to the reaction between Na_2CO_3 and Nb_2O_5. In order to deepen our knowledge of the mechanisms of mechanochemical reactions and make general conclusions, further studies on other systems are necessary. The aim of the present work is to gain an insight into the mechanism of the mechanochemical synthesis of $KNbO_3$ from a K_2CO_3–Nb_2O_5 powder mixture. To make comparisons, the milling parameters were set so that the mechanochemical reaction occurred at different ball-impact energies, i.e., 35 and 300 mJ/hit. X-ray diffraction, thermogravimetric analysis, and infrared and Raman spectroscopy were used to follow the reaction.

2. Experimental

The mechanochemical synthesis of $KNbO_3$ was performed starting from an equimolar mixture of K_2CO_3 (99+%, Aldrich) and Nb_2O_5 (99.9%, Aldrich). Because of its hygroscopic nature the K_2CO_3 powder was dried at 200 °C before use. After weighing, the two powders were placed into the vial and subjected to high-energy milling. The powder masses for the high-energy milling experiments are given in Table 1. A mixture of K_2CO_3 and Nb_2O_5, subsequently referred to as the non-milled mixture, was prepared by mixing the constituents in an agate mortar using acetone. $KNbO_3$ prepared by a conventional solid-state synthesis route was used as a reference. The synthesis was carried out by first mixing an equimolar mixture of K_2CO_3 and Nb_2O_5 in an attritor mill in acetone at 800 min^{-1} for 4 h using YSZ (yttria-stabilized zirconia) milling balls with a diameter of 3 mm. The $KNbO_3$ powder was then obtained by double calcination at 650 °C for 4 h with an intermediate wet-milling step.

The high-energy milling was performed using two planetary mills, i.e., a Retsch PM400 and a Fritsch Pulverisette 4 Vario-Mill. The milling parameters, the ball-impact energy and the ball-impact frequency for the two experiments are summarized in Table 1. The ball-impact energy and the ball-impact frequency were calculated from the milling parameters, using the models originally derived by Burgio et al.[18] for metal systems and subsequently applied to the mechanochemical synthesis of ceramic oxides.[16]

In addition to the milling experiments performed under usual atmospheric conditions, we also milled the K_2CO_3–Nb_2O_5 mixture under dry conditions at 300 mJ/hit of ball-impact energy. This was accomplished by weighing the powders and filling the milling vial in a dry box. To assure dry conditions during high-energy milling we used a cover for the vial, which we modified to allow only outlet of gases evolved during the reaction (in this case CO_2). The sampling was performed in the dry box.

X-ray powder-diffraction (XRD) analyses were made with a Siemens D5000 and a Panalitical X'Pert PRO diffractometer, both operating with Cu Kα radiation. The data were collected in the 2-theta range from 20° to 70° with a step size of 0.04° and an acquisition time of 2 s/step (Siemens) or a step of 0.017° per 100 s and a fully opened X'Celerator detector (Panalitical). The XRD pattern of the K_2CO_3–Nb_2O_5 non-milled mixture was recorded while the powder was covered with a polymeric foil.

Thermogravimetric (TG) analyses were made using a NETZSCH STA 409 analyzer. Around 50 mg of powder was placed in a Pt/Rh crucible and heated up to 900 °C with a heating rate of 10 °C/min. The measurements were performed in an atmosphere of flowing air. A simultaneous evolved-gas analysis (EGA) for H_2O and CO_2 using a Balzers Thermostar GSD 300 T mass spectrometer was also performed.

The infrared spectra were recorded using a PerkinElmer Spectrum 100 FT-IR spectrometer, equipped with a Specac Golden Gate Diamond ATR as a sample support. The data were collected in the wavenumber range 600–4000 cm^{-1} with a spectral resolution of 2 cm^{-1} and 4 scans.

FT-NIR Raman spectra were recorded using a Bruker IFS66FRA106 spectrometer. The samples were excited with a 1064-nm diode-pumped Nd:YAG laser. Raman scattering studies were carried out using a 180° geometry and recorded in the 100–1200 cm^{-1} wavenumber range. The data were collected with 500 or 1000 scans and a 2 cm^{-1} spectral resolution.

The samples were analyzed by an analytical transmission electron microscope (TEM) JEM 2010F FEG-AEM, operated at 200 kV of accelerating voltage. The chemical composition was determined using a LINK ISIS 300 energy-dispersive X-ray spectrometer (EDXS).

3. Results and discussion

3.1. Ball-impact energy 35 mJ/hit

Fig. 1 shows the XRD patterns of the non-milled K_2CO_3–Nb_2O_5 mixture and after 20, 90, 110 and 150 h of milling. The non-milled mixture is composed of monoclinic K_2CO_3[19] and orthorhombic Nb_2O_5.[20] 20 h of milling lead to a complete amorphisation of the K_2CO_3, which is consistent also with the high background observed on the XRD pattern. The Nb_2O_5 is still present in the mixture; however, its crystallite size is

Table 1
Milling parameters, ball-impact energy and ball-impact frequency.

Planetary mill	R_p (cm)	Milling vial	Milling balls	Rotational frequency W_p (min^{-1})	Powder mass (g)	Ball-impact energy (mJ/hit)	Ball-impact frequency (s^{-1})
Retsch PM400	15	125 ml YSZ	40 YSZ (10 mm)	300	5	35	600
Fritsch Pulverisette 4	12	250 ml WC	16 WC (15 mm)	270	10	300	320

R_p is the distance between the rotational axes of the supporting disc and the milling vial. W_p is the rotational frequency of the supporting disc. The vial's rotational frequency W_v in both experiments is twice the supporting disc's rotational frequency, or $W_v = 2W_p$. YSZ refers to yttria-stabilized zirconia and WC to tungsten carbide. The diameters of the YSZ and WC cylindrical milling vials are 6 and 7.5 cm, and the heights are 4.4 and 5.7 cm, respectively. The densities of YSZ and WC are 6.3 and 15.1 g/cm^3, respectively (the ball diameter is given in brackets). The ball-impact energy and the ball-impact frequency are calculated according to.[16,18]

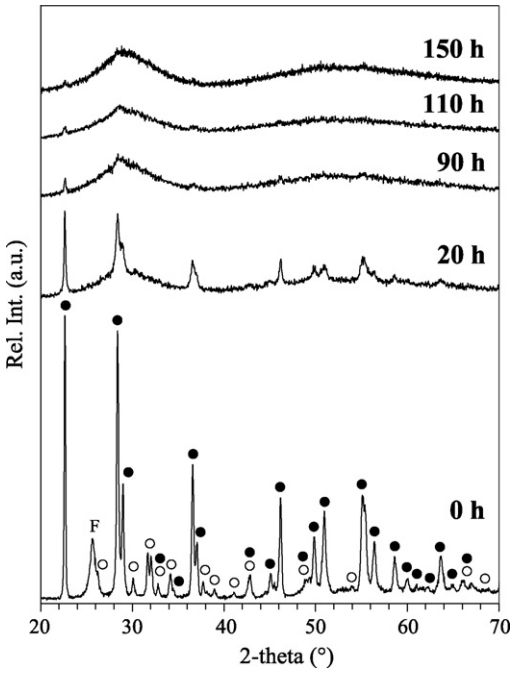

Fig. 1. XRD patterns of non-milled K_2CO_3–Nb_2O_5 mixture (0 h) and after milling at 35 mJ/hit of ball-impact energy for 20, 90, 110 and 150 h (notation: (◯) K_2CO_3, (●) Nb_2O_5, (F) foil).

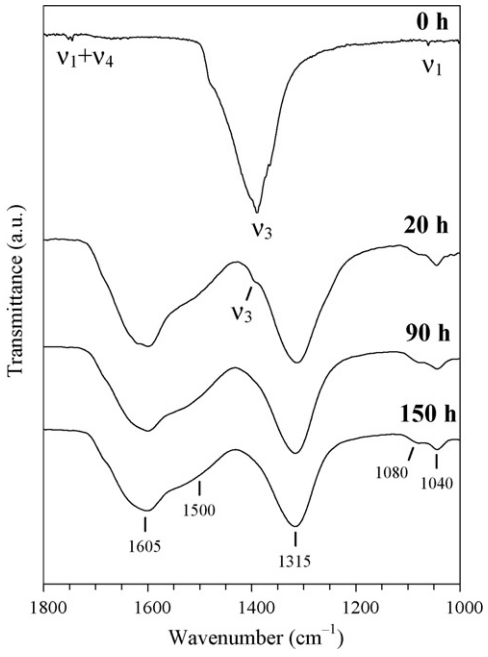

Fig. 2. IR spectra of non-milled K_2CO_3–Nb_2O_5 mixture (0 h) and after milling at 35 mJ/hit of ball-impact energy for 20, 90 and 150 h (ν_1, ν_3 and ν_4 denote CO_3^{2-} vibrations).

reduced, which is evident from the peak broadening. With further milling the amount of crystalline Nb_2O_5 gradually decreases, and an almost complete amorphisation of the mixture is achieved after 150 h. It can be noted that the main part of the amorphisation process of Nb_2O_5 occurs in the initial 90 h of milling, after which it proceeds slowly, suggesting that the reaction approaches a steady condition, similarly as observed for the mechanochemical synthesis of $NaNbO_3$.[17]

Table 2 summarizes the results of the TG analyses on the powder mixtures milled for 20 and 150 h. The amount of H_2O, which accumulates during milling from the moisture present in the environment, is 6.0% after 20 h, and the value does not change after 150 h of milling. From the amount of CO_2 released upon heating the samples to 900 °C, we were also able to calculate the fraction of phase equivalent to K_2CO_3, taking into account the theoretical CO_2 loss for the carbonate decomposition in a K_2CO_3–Nb_2O_5 1:1 molar mixture (10.9%). It should be noted that even after 150 h of milling the majority of the carbonate phase, i.e., 90%, is still present in the mixture in an amorphous state.

The coordination state of the carbonate ions (CO_3^{2-}) was further examined by IR spectroscopy (Fig. 2). The spectrum of the non-milled mixture (0 h) can be fully described with vibrations typical for the free CO_3^{2-} ion: an asymmetrical C–O stretching vibration around 1400 cm^{-1} (ν_3), a symmetrical C–O stretching vibration at 1060 cm^{-1} (ν_1) and a combinational mode of the type $\nu_1 + \nu_4$ around 1750 cm^{-1}.[21,22] The ν_1 vibration is IR-inactive for the free CO_3^{2-} ion and also for some simple carbonates, including Na_2CO_3, as shown in our previous work.[15] However, it appears as a weak band in K_2CO_3 (Fig. 2, 0 h). This is due to a small distortion of the CO_3^{2-} ion from its D_{3h} structure due to the presence of K^+ ions.[23,24] Upon milling, substantial changes can be observed in the IR spectra. The ν_3 vibration is present as a weak band after 20 h, but it disappears with further milling; it splits into three absorption bands, which appear at 1605, 1500 and 1315 cm^{-1}. The ν_1 vibration splits into two bands at 1080 and 1040 cm^{-1} with increased intensity. The splitting of the ν_3 and the increase in the intensity of the ν_1 vibration are characteristic for a lowering of the CO_3^{2-} structural symmetry, which is in turn related to the coordination of the CO_3^{2-} ions into a carbonato complex.[22] In addition, the splitting of ν_1 is also observed in many carbonato complexes and probably arises from the interaction of neighbouring groups. There are a large number of complexes reported in the literature with metals such as Co and Cu having characteristic bands that are in a good agreement with the observed from Fig. 2. An example is the $Na_2Cu(CO_3)_2$ complex for which the structure has been

Table 2
Mass losses due to H_2O and CO_2 release upon heating the milled samples (20 and 150 h) to 900 °C (ball-impact energy 35 mJ/hit). The temperature ranges of H_2O and CO_2 release and the calculated fraction of K_2CO_3 are also given.

Milling time (h)	Mass loss—H_2O (%)	Mass loss—CO_2 (%)	Fraction of K_2CO_3[a] (%)
20	6.0% (25–265 °C)	10.3% (265–900 °C)	100
150	6.0% (25–275 °C)	9.2% (275–900 °C)	90

[a] Refers to the fraction of the phase equivalent to the K_2CO_3 present in the sample.

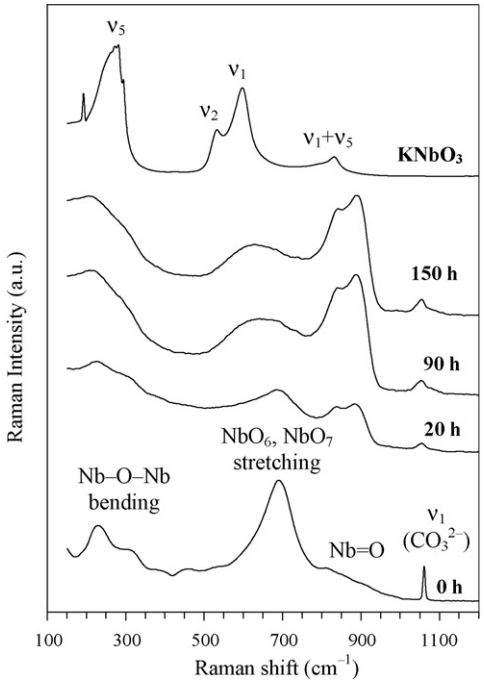

Fig. 3. Raman spectra of non-milled K_2CO_3–Nb_2O_5 mixture (0 h) and after milling at 35 mJ/hit of ball-impact energy for 20, 90 and 150 h. The spectrum of $KNbO_3$ is added for comparison (ν_1, ν_2 and ν_5 denote NbO_6 vibrational modes).

determined using single-crystal X-ray diffraction methods and it is characterized by bridged coordinated carbonate ions.[25] In our case, based on the fact that we did not observe any new crystalline phases during 150 h of milling (Fig. 1), the complex is amorphous, or eventually nanocrystalline, to an extent to which it is undetectable with X-ray diffraction methods. The formation of a carbonato complex, which occurs simultaneously with the amorphisation of the carbonate, was also observed in the Na_2CO_3–Nb_2O_5 system.[15]

Fig. 3 shows the Raman spectra of the non-milled K_2CO_3–Nb_2O_5 mixture (0 h) and mixtures after 20, 90 and 150 h of milling. The spectrum of $KNbO_3$ is added for comparison. Here, the Raman bands can be ascribed to the internal vibrational modes of the NbO_6 octahedra, i.e., ν_1 (A_{1g}), ν_2 (E_g) and ν_5 (F_{2g}).[26] The first two are stretching and the last one bending mode. The weak band at 830 cm^{-1} corresponds to the $\nu_1 + \nu_5$ combinational band. The spectrum of the non-milled mixture (0 h) can be described as follows: the sharp band at 1060 cm^{-1} belongs to the symmetrical C–O stretching vibration of the CO_3^{2-} ion in K_2CO_3 (ν_1), which was also observed in the IR spectrum (Fig. 2), and appears as the most intense band in the Raman spectrum of pure K_2CO_3[23]; the other bands are related to Nb_2O_5, i.e., the broad band at 680 cm^{-1} belongs to the symmetrical stretching mode of the NbO_6 and NbO_7 units present in the orthorhombic Nb_2O_5, the group of bands in the low-wavenumber region (150–350 cm^{-1}) belong to the bending modes of the Nb–O–Nb linkages and the broad Raman band around 900 cm^{-1} is related to the terminal Nb=O bonds present as surface species.[27]

After 20 h of milling the band at 680 cm^{-1} and the group of bands in the region 150–350 cm^{-1} broaden, showing a more disordered Nb_2O_5 structure. New bands appear in the wavenumber region 800–950 cm^{-1}. With further milling from 20 to 150 h, the intensities of these bands increase. At the same time, two broad bands appear in the regions 150–350 cm^{-1} and 500–750 cm^{-1}, both shifted in comparison with the ν_5 and ν_1 bands of $KNbO_3$, respectively. The ν_1 (CO_3^{2-}) vibration splits into two components, one being broader, which was also observed for the IR spectra (Fig. 2).

Jehng and Wachs[27] studied in detail a number of niobium oxide compounds, giving a general relationship between the observed Raman spectra and their structures. The large majority of the niobium compounds contain NbO_6 octahedra with different degrees of distortion. For slightly distorted corner-shared octahedra with Nb–O bond lengths typically around 2 Å, present, for example, in perovskites such as $KNbO_3$ and $NaNbO_3$, the major Raman bands appear in the wavenumber region 500–700 cm^{-1}. On the other hand, highly distorted octahedra exhibit bands at higher wavenumbers, i.e., 850–1000 cm^{-1}. The distortion of the NbO_6 octahedra can be due to non-bridging oxygens, such as those found in layered structures, and/or due to common oxygens shared by two or more NbO_6 octahedra, both leading to shorter Nb–O bonds than those in perovskites.[28–30] Therefore, the broad Raman band, which appears during milling in the region 500–750 cm^{-1} (Fig. 3), indicates the formation of slightly distorted NbO_6 octahedra, while the bands at higher wavenumbers (800–950 cm^{-1}) could be related to a more distorted octahedra or shorter Nb–O bonds. It seems that both are characterized by short-range ordering, since no formation of crystalline phases is observed during milling up to 150 h, while two broad bumps are observed on the XRD patterns (Fig. 1).

3.2. Ball-impact energy 300 mJ/hit

The XRD patterns of the non-milled K_2CO_3–Nb_2O_5 mixture (0 h) and after 20, 90, 150 and 350 h of milling are shown in Fig. 4. From 0 to 90 h the same reaction course is observed as in the case of the 35 mJ/hit of ball-impact energy (Fig. 1), i.e., complete amorphisation of the K_2CO_3 and a progressive decrease in the amount of crystalline Nb_2O_5. However, in contrast to the low-energy experiment, new broad peaks appear after 150 h at 2-theta equal to 22.5°, 31.5°, 45.5°, 48.5°, 51.2°, 56.3° and 65.5°, which can be assigned to $KNbO_3$[31] and $K_6Nb_{10.88}O_{30}$.[32] With additional milling, further crystallization takes place. The XRD pattern after 350 h can be best described with $KNbO_3$, $K_8Nb_{18}O_{49}$[33] and $K_6Nb_{10.88}O_{30}$, the last of these being the predominant phase. The small peaks at 33.8°, 44.3° and 57.5° could not be identified.

For comparison, we added in Fig. 4 also the XRD pattern of Nb_2O_5, which was milled separately for 90 h applying 300 mJ/hit of ball-impact energy. The extent of the amorphisation of the oxide when milled separately is much lower than in the case of milling with K_2CO_3 for the same period of treatment, i.e., 90 h. This clearly shows that the amorphisation does not originate simply from the highly energetic ball collisions acting on the powder but it is driven by the mechanochemical reaction with K_2CO_3.

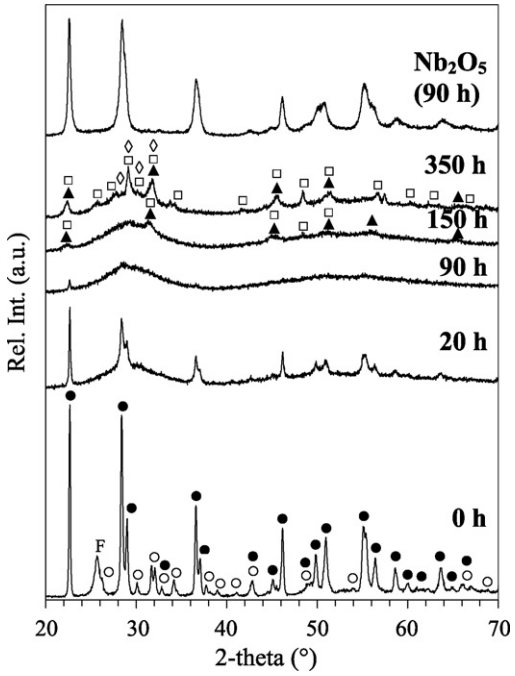

Fig. 4. XRD patterns of non-milled K_2CO_3–Nb_2O_5 mixture (0 h) and after milling at 300 mJ/hit of ball-impact energy for 20, 90, 150 and 350 h (notation: (◯) K_2CO_3, (●) Nb_2O_5, (▲) $KNbO_3$, (□) $K_6Nb_{10.88}O_{30}$, (◊) $K_8Nb_{18}O_{49}$, (F) foil). The pattern of Nb_2O_5 milled separately for 90 h is given for comparison.

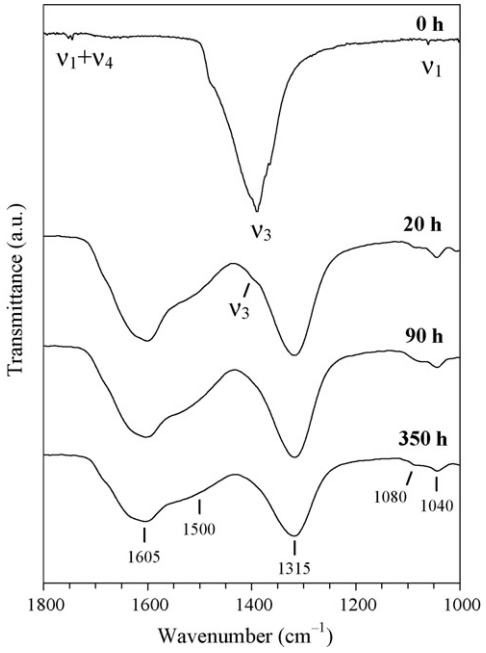

Fig. 5. IR spectra of non-milled K_2CO_3–Nb_2O_5 mixture (0 h) and after milling at 300 mJ/hit of ball-impact energy for 20, 90 and 350 h (ν_1, ν_3 and ν_4 denote CO_3^{2-} vibrations).

Table 3 shows the results of the TG analyses on the powders milled for 20 and 350 h. The amount of accumulated water is 6.3% after 20 h, which slightly decreases to 5.2% after 350 h of milling. Almost all of the carbonate is present in the mixture after 20 h, i.e., 98%, while it decomposes partially after 350 h (72%). At the same time we observe the crystallization of the niobate phases (Fig. 4, 350 h).

According to the concept of soft mechanochemistry, H_2O accumulated during milling might have an important influence on the course of the mechanochemical reaction through possible acid–base reactions between dissimilar particles.[14] We verified its effect by milling the mixture in dry conditions as described in the experimental section. In terms of reaction course, i.e., amorphisation of the mixture and formation of niobate phases, there were no substantial differences in comparison with the experiment carried out under atmospheric conditions.

Fig. 5 shows the IR spectra of the non-milled (0 h) and milled K_2CO_3–Nb_2O_5 mixtures (20, 90, and 350 h). The ν_3 vibration of the CO_3^{2-} ion disappears with increasing milling time, like we observed in the case of the 35 mJ/hit of ball-impact energy (Fig. 2). In this region new absorption bands appear at 1605, 1500 and 1315 cm^{-1}, and the ν_1 vibration splits into two bands at 1080 and 1040 cm^{-1}. The same changes were observed at 35 mJ/hit (Fig. 2), showing that a carbonato complex also forms with a higher ball-impact energy.

Fig. 6 shows the Raman spectra of the non-milled K_2CO_3–Nb_2O_5 mixture (0 h) and after 20, 90 and 350 h of milling, together with the spectrum of $KNbO_3$ as a reference. Like in the case of 35 mJ/hit (Fig. 3, 20 h), broadening of the bands at 680 cm^{-1} and 150–350 cm^{-1} is first observed after 20 h of milling, together with the appearance of Raman bands in the region 800–950 cm^{-1}. After 90 h of milling a broad Raman band, which was also observed at 35 mJ/hit (Fig. 3, 90 h), appears in the region 500–750 cm^{-1}. However, in contrast to the low-energy experiment, with increasing milling time from 90 to 350 h the intensities of the high-wavenumber bands (800–950 cm^{-1}) decrease, while the band in the region 500–750 cm^{-1} sharpens. These changes are related to the crystallization of the niobate phases (Fig. 4, 350 h), which means that the sharpening of the band in the region 500–750 cm^{-1} corresponds to the long-range ordering of the slightly distorted corner-shared NbO_6 octahedra present in both $KNbO_3$[34] and $K_6Nb_{10.88}O_{30}$.[35] Furthermore, the formation of the niobate phases during milling occurs via an

Table 3
Mass losses due to H_2O and CO_2 release upon heating the milled samples (20 and 350 h) to 900 °C (ball-impact energy 300 mJ/hit). The temperature ranges of H_2O and CO_2 release and the calculated fraction of K_2CO_3 are also given.

Milling time (h)	Mass loss—H_2O (%)	Mass loss—CO_2 (%)	Fraction of K_2CO_3[a] (%)
20	6.3% (25–270 °C)	10.0% (270–900 °C)	98
350	5.2% (25–275 °C)	7.4% (275–900 °C)	72

[a]Refers to the fraction of the phase equivalent to the K_2CO_3 present in the sample.

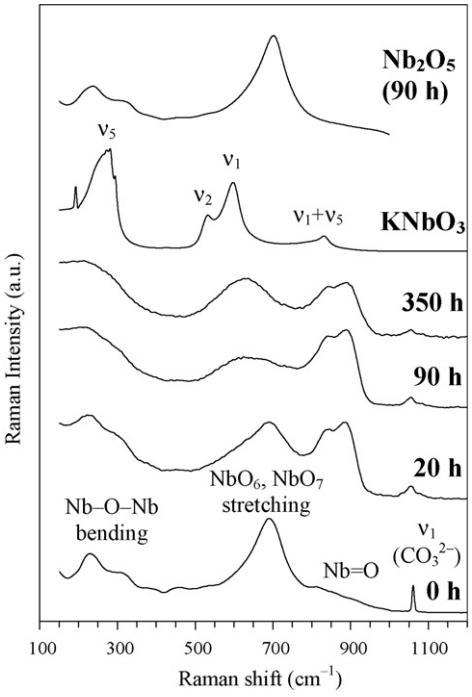

Fig. 6. Raman spectra of non-milled K_2CO_3–Nb_2O_5 mixture (0 h) and after milling at 300 mJ/hit of ball-impact energy for 20, 90 and 350 h. The spectra of $KNbO_3$ and 90-h-milled Nb_2O_5 are added for comparison (ν_1, ν_2 and ν_5 denote NbO_6 vibrational modes).

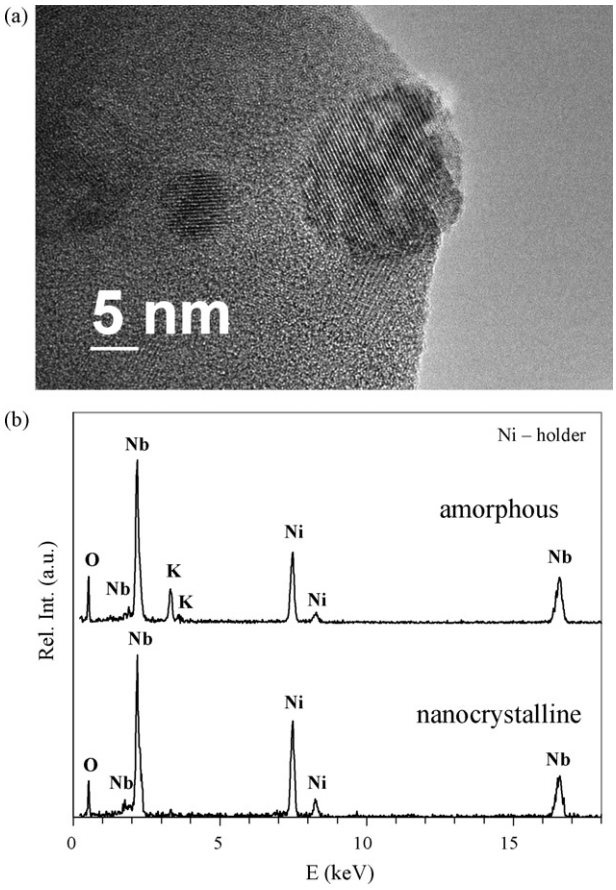

Fig. 7. (a) TEM image of the K_2CO_3–Nb_2O_5 mixture milled for 90 h and (b) EDXS spectra taken from nanocrystalline and amorphous regions.

intermediate phase, characterized by shorter Nb–O bonds than those in corner-shared octahedra (~2 Å) with Raman bands in the 800–950 cm^{-1} region. The decrease in the intensity of these bands from 90 to 350 h of milling occurs simultaneously with the decrease in the intensity of the bands in the ν_1 (CO_3^{2-}) region. This suggests that they could be related to the bonding in the carbonato complex. To confirm this, we also milled Nb_2O_5 separately. In this case, the bands in the 800–950 cm^{-1} region do not appear after 90 h of milling. The short Nb–O bonds are therefore formed during the reaction with K_2CO_3 and are related to the carbonato complex.

The 90-h-milled K_2CO_3–Nb_2O_5 mixture was also investigated using TEM (Fig. 7). The powder was found to be amorphous with nanocrystallites embedded into the amorphous matrix (Fig. 7a). Based on the EDXS analysis (Fig. 7b), these nanocrystallites are Nb_2O_5, confirming the results of XRD (Fig. 4, 90 h). In the amorphous phase both K and Nb were detected confirming the reaction between K_2CO_3 and Nb_2O_5 during mechanochemical treatment.

3.3. Comparison with the Na_2CO_3–Nb_2O_5 system

In order to advance in the study of the mechanisms involved during a mechanochemical reaction comparison between different systems is essential. On the basis of the results, the mechanochemical reaction between K_2CO_3 and Nb_2O_5 can be summarized as follows: in the first place, a carbonato complex forms as a result of the mechanochemical interaction between the two reagents. This process requires the rearrangement of the CO_3^{2-} ions from the original structure, which is realized through the amorphisation of K_2CO_3. The same phenomenon was also observed in the Na_2CO_3–Nb_2O_5 system,[15] leading to a conclusion that the mechanochemical interaction between alkaline carbonates (Na_2CO_3, K_2CO_3) and Nb_2O_5 is governed by the same mechanism. However, some important differences should be emphasized, such as the stability of the carbonato complex under high-energy ball impacts. In the Na_2CO_3–Nb_2O_5 system, 70% of the complex decomposes after 16 h of milling when 370 mJ/hit and 360 s^{-1} of ball-impact energy and ball-impact frequency are applied.[17] In contrast, if K_2CO_3 and Nb_2O_5 are milled under comparable conditions (300 mJ/hit, 320 s^{-1}), only 28% of the complex decomposes after 350 h of milling (Table 3). Such a large difference is also reflected in the crystallization of phases during milling, for which the decomposition of the carbonate is necessary. The critical cumulative kinetic energy (weight-normalized product of the ball-impact energy, the ball-impact frequency and the milling time) for the formation of $NaNbO_3$ from a Na_2CO_3–Nb_2O_5 mixture was determined to be between 7 and 12 kJ/g.[16] Taking into account the results of the present study, one can calculate a cumulative kinetic energy of 5200 kJ/g for the crystallization of niobate phases at 300 mJ/hit. A further particularity of the mechanochemical reaction between K_2CO_3 and Nb_2O_5 in comparison with the Na_2CO_3–Nb_2O_5 system, is the formation of niobate phases with a molar ratio K/Nb < 1. At present we are not able to give an explanation for

such a difference, and further investigations on other systems are going to be necessary. However, we can conclude that the formation of these phases occurs via the long-range ordering of the NbO_6 octahedra, already formed in the initial stage of the milling.

4. Conclusions

The mechanism of the mechanochemical reaction between K_2CO_3 and Nb_2O_5 was studied using X-ray diffraction, thermogravimetric analysis, infrared spectroscopy and Raman spectroscopy. The reaction was carried out with two different ball-impact energies, i.e., 35 and 300 mJ/hit. Based on the results, we can draw the following conclusions:

1. Irrespective of the ball-impact energy applied, K_2CO_3 and Nb_2O_5 react to form an amorphous carbonato complex, which represents an intermediate stage of the mechanochemical reaction. The associated coordination of the CO_3^{2-} ions is realized through the amorphisation of K_2CO_3. The complex was identified by both the decrease of the symmetry of the initial CO_3^{2-} ions and the formation of new Nb–O bonds.
2. At 35 mJ/hit of ball-impact energy only a minor fraction of the carbonato complex decomposes after 150 h of milling, i.e., 10%, and no formation of $KNbO_3$ is observed. However, short-range ordering of the NbO_6 octahedra, those typically encountered in some potassium niobate structures such as $KNbO_3$ and $K_6Nb_{10.88}O_{30}$, takes place.
3. The carbonato complex decomposes to a larger extent after prolonged milling (28%, 350 h) by applying higher ball-impact energy, i.e., 300 mJ/hit. This leads to the crystallization of $KNbO_3$ and other niobate phases with $K/Nb < 1$, which occurs through the long-range ordering of the NbO_6 octahedra, already formed in the initial stage of milling and also observed at 35 mJ/hit of ball-impact energy.

Acknowledgements

This work was supported by the Slovenian Research Agency and was carried out as part of the postdoctoral project "Mechanochemical synthesis of complex ceramic oxides" (Z2-1195). The Raman scattering studies were performed as part of a short-term scientific mission (STSM) financed by the European Cooperation in the field of Scientific and Technical Research (COST Action 539). We would like to thank Mr. Edi Kranjc for recording the X-ray diffraction patterns. Ms. Jana Cilenšek is acknowledged for help in the preparation of the samples for thermal analysis and Dr. Bojan Kozlevčar for the support given in recording the infrared spectra.

References

1. Shrout, T. R. and Zhang, S. J., Lead-free piezoelectric ceramics: Alternatives for PZT? *J. Electroceram.*, 2007, **19**, 111–124.
2. Malič, B., Bernard, J., Holc, J., Jenko, D. and Kosec, M., Alkaline-earth doping in (K, Na)NbO_3 based piezoceramics. *J. Eur. Ceram. Soc.*, 2005, **25**, 2707–2711.
3. Wang, Y., Damjanovic, D., Klein, N., Hollenstein, E. and Setter, N., Compositional inhomogeneity in Li- and Ta-modified (K,Na)NbO_3 ceramics. *J. Am. Ceram. Soc.*, 2007, **90**, 3485–3489.
4. Skidmore, T. A. and Milne, S. J., Phase development during mixed-oxide processing of a $[Na_{0.5}K_{0.5}]_{1-x}[LiTaO_3]_x$ powder. *J. Mater. Res.*, 2007, **22**, 2265–2272.
5. Stojanović, B. D., Mechanochemical synthesis of ceramic powders with perovskite structure. *J. Mater. Process. Technol.*, 2003, **143–144**, 78–81.
6. Wang, J., Xue, J. M., Wan, D. M. and Gan, B. K., Mechanically activating nucleation and growth of complex perovskites. *J. Solid State Chem.*, 2000, **154**, 321–328.
7. Xue, J. M., Wan, D. M. and Wang, J., Functional ceramics of nanocyrstallinity by mechanical activation. *Solid State Ionics*, 2002, **151**, 403–412.
8. Kuscer, D., Holc, J. and Kosec, M., Mechano-synthesis of lead-magnesium-niobate ceramics. *J. Am. Ceram. Soc.*, 2006, **89**, 3081–3088.
9. Kuscer, D., Holc, J. and Kosec, M., Formation of 0.65 $Pb(Mg_{1/3}Nb_{2/3})O_3$–0.35 $PbTiO_3$ using high-energy milling process. *J. Am. Ceram. Soc.*, 2007, **90**, 29–35.
10. Zyryanov, V. V., Ultrafast mechanochemical synthesis of mixed oxides. *Inorg. Mater.*, 2005, **41**, 378–392.
11. Liao, J. and Senna, M., Enhanced dehydration and amorphization of $Mg(OH)_2$ in the presence of ultrafine SiO_2 under mechanochemical conditions. *Thermochim. Acta*, 1992, **210**, 89–102.
12. Liao, J. and Senna, M., Mechanochemical dehydration and amorphization of hydroxides of Ca, Mg and Al on grinding with and without SiO_2. *Solid State Ionics*, 1993, **66**, 313–319.
13. Watanabe, T., Isobe, T. and Senna, M., Mechanisms of incipient chemical reaction between $Ca(OH)_2$ and SiO_2 under moderate mechanical stressing. I: a solid state acid–base reaction and charge transfer due to complex formation. *J. Solid State Chem.*, 1996, **122**, 74–80.
14. Avvakumov, E., Senna, M. and Kosova, N., *Soft Mechanochemical Synthesis*. Kluwer Academic Publishers, Boston, 2001.
15. Rojac, T., Kosec, M., Šegedin, P., Malič, B. and Holc, J., The formation of a carbonato complex during the mechanochemical treatment of a Na_2CO_3–Nb_2O_5 mixture. *Solid State Ionics*, 2006, **177**, 2987–2995.
16. Rojac, T., Kosec, M., Malič, B. and Holc, J., The application of a milling map in the mechanochemical synthesis of ceramic oxides. *J. Eur. Ceram. Soc.*, 2006, **26**, 3711–3716.
17. Rojac, T., Kosec, M., Malič, B. and Holc, J., The mechanochemical synthesis of $NaNbO_3$ using different ball-impact energies. *J. Am. Ceram. Soc.*, 2008, **91**, 1559–1565.
18. Burgio, N., Iasonna, A., Magini, M., Martelli, S. and Padella, F., Mechanical alloying of the Fe–Zr system. Correlation between input energy and end products. *Il Nuovo Cimento*, 1990, **13D**, 459–476.
19. K_2CO_3, Powder diffraction file 71-1466 (PDF-2 database).
20. Nb_2O_5, Powder diffraction file 27-1313 (PDF-2 database).
21. Brooker, M. H. and Hates, J. B., Raman and infrared spectral studies of anhydrous potassium and rubidium carbonate. *Spectrochim. Acta*, 1974, **30A**, 2211–2220.
22. Gatehouse, B. M., Livingstone, S. E. and Nyholm, R. S., The infrared spectra of some simple and complex carbonates. *J. Chem. Soc.*, 1958, 3137–3142.
23. Koura, N., Kohara, S., Takeuchi, K., Takahashi, S., Curtiss, L. A., Grimsditch, M. and Saboungi, M. L., Alkali carbonates: Raman spectroscopy, ab initio calculations, and structure. *J. Mol. Struct.*, 1996, **382**, 163–169.
24. Schutte, C. J. H. and Buijs, K., The infra-red spectra of K_2CO_3 and its hydrates. *Spectrochim. Acta*, 1961, **17**, 921–926.
25. Healy, P. C. and White, A. H., Crystal structure and physical properties of anhydrous sodium copper carbonate. *J. Chem. Soc. Dalton Trans.*, 1972, 1913–1917.
26. Kakimoto, K., Akao, K., Guo, Y. and Ohsato, H., Raman scattering study of piezoelectric $(Na_{0.5}K_{0.5})NbO_3$–$LiNbO_3$ ceramics. *Jpn. J. Appl. Phys.*, 2005, **44**, 7064–7067.
27. Jehng, J. M. and Wachs, I. E., Structural chemistry and Raman spectra of niobium oxides. *Chem. Mater.*, 1991, **3**, 100–107.
28. McConnell, A. A., Raman spectra of niobium oxides. *Spectrochim. Acta*, 1976, **32A**, 1067–1076.

29. Fukumi, K. and Sakka, S., Coordination state of Nb^{5+} ions in silicate and gallate glasses as studied by Raman spectroscopy. *J. Mater. Sci.*, 1988, **23**, 2819–2823.
30. Fukumi, K., Kokubo, T., Kamiya, K. and Sakka, S., Structures of alkali niobium gallate glasses. *J. Non-Cryst. Solids*, 1986, **84**, 100–104.
31. $KNbO_3$, Powder diffraction file 71-0946 (PDF-2 database).
32. $K_6Nb_{10.88}O_{30}$, Powder diffraction file 87-1856 (PDF-2 database).
33. $K_8Nb_{18}O_{49}$, Powder diffraction file 31-1065 (PDF-2 database).
34. $KNbO_3$, Inorganic crystal structure database (ICSD) N°14363.
35. $K_6Nb_{10.8}O_{30}$, Inorganic crystal structure database (ICSD) N°409464.